Characterization of the S272A,D Site-Directed Mutations of *O*-Acetylserine Sulfhydrylase: Involvement of the Pyridine Ring in the α,β-Elimination Reaction†

Sebastian Daum,‡ Chia-Hui Tai,§ and Paul F. Cook*

Department of Chemistry and Biochemistry, University of Oklahoma, 620 Parrington Oval, Norman, Oklahoma 73072

Received September 5, 2002; Revised Manuscript Received November 12, 2002

ABSTRACT: *O*-Acetylserine sulfhydrylase catalyzes the synthesis of L-cysteine from *O*-acetyl-L-serine (OAS) and inorganic bisulfide. An anti-E_2 mechanism has been proposed for the OASS-catalyzed elimination of acetate from OAS (Tai, C.-H., and Cook, P. F. (2001) *Acc. Chem. Res. 34*, 49−59). Site-directed mutagenesis was used to change S272 to alanine, which would be expected to eliminate the hydrogen bond to N1 of PLP or to aspartate, which would be expected to enhance the hydrogen-bonding interaction. Both mutant enzymes catalyze the overall reaction and are in fact still good enzymes, consistent with the proposed anti-E_2 mechanism. Data suggest that hydrogen bonding to the pyridine ring does not play a significant role in the α,β-elimination reaction catalyzed by OASS-A. The V/K_{OAS}, which reflects the first half-reaction, is identical to the wild-type enzyme in the case of the S272D mutant enzyme and is decreased by only a factor of 3 in the case of the S272A mutant enzyme. In the case of the alanine mutation, and to a lesser extent the aspartate mutation, a decrease in the rate of the elimination is compensated by an increase in affinity for OAS, leading to the observed second-order rate constant, *V*/*K*. The decrease in the rate of the elimination is proposed to result from a change in the orientation of the bound cofactor, as might be expected since one of the ligands that determines the position of the bound PLP has been changed. Consistent with a change in the orientation of the cofactor are the results from a number of the spectral probes. The visible CD data for the internal Schiff base have a molar ellipticity 50% that of wild-type enzyme, and the α-aminoacrylate intermediate has a molar ellipticity 25% that of wild-type enzyme. The α-aminoacrylate intermediate can be formed from L-cysteine and L-serine with the S272A,D mutant enzymes, but not with the wild-type enzyme, and taken together with the increased K_d for the serine external Schiff base is consistent with a change in cofactor orientation in the active site. The long wavelength fluorescence emission for the S272A mutant enzyme, attributed to Förster resonance energy transfer (McClure, G. D., Jr., and Cook, P. F. (1994) *Biochemistry 33*, 1647−1683) has an intensity near zero, as compared to significant fluorescence for the wild-type enzyme.

O-Acetylserine sulfhydrylase (OASS)[1] catalyzes the PLP-dependent replacement of the β-acetoxy of OAS by inorganic bisulfide to generate L-cysteine, Scheme 1 (*1*). The mature protein is composed of two identical subunits, each of which comprises 315 amino acid residues. The three-dimensional structure of the 68 900 Da OASS-A has been solved to 2.2 Å (*2*). A subunit of OASS-A has two domains, a N-terminal domain and a C-terminal domain, each of which contains roughly half of the amino acids in the overall protein. Each single subunit of the OASS-A dimer has one distinct active site, located deep within the protein, at the interface of the N- and C-terminal domains of each subunit.

The PLP cofactor in the active site is in Schiff base linkage with the ε-amino group of K41 of OASS-A, Figure 1 (*3*). Additionally, several hydrogen bonds stabilize the cofactor. The 5′-phosphate of PLP is tightly hydrogen-bonded to residues G176 through T180, while N71 donates a hydrogen bond to O3′ of the cofactor (*2*). Unlike the α family of PLP-dependent enzymes, which have an aspartate hydrogen-bonded to N1 of the PLP pyridine ring, S272 is thought to donate a hydrogen bond to the ring-nitrogen of PLP in OASS-A.

In most of the known PLP-dependent enzymes in which the PLP is used for amino acid metabolism, the pyridine ring functions as an electron-withdrawing group. The ring is thought to be crucial for acidifying the α-proton and for stabilizing the carbanion that is produced after the general base abstracts the α-proton. In PLP-dependent α,β-elimination reactions, the mechanism is thought to proceed via an E_1cB reaction in which a quinonoid is a stable intermediate, while the intermediate would not be formed in an E_2 reaction, Scheme 2.

† This work was supported by a grant to P.F.C. from the National Science Foundation (MCB 0111024) and by an endowment on behalf of Grayce B. Kerr to the University of Oklahoma. A preliminary version of this work has been published previously (Cook, P. F. (2002) *Biochim. Biophys. Acta*, accepted).

* Corresponding author: Tel: (405) 325-4581. Fax: (405) 325-7182. E-mail: pcook@chemdept.chem.ou.edu.

‡ Present address: Max Planck Forschungsstelle für Enzymologie der Proteinfaltung, Weinbergweg 22, 06120 Halle (Saale), Germany.

§ Present address: Department of Chemical Engineering, Chenshiu Institute of Technology, Kaohsiung, Taiwan, Republic of China.

[1] Abbreviations: OASS-A, the A-isozyme of *O*-acetylserine sulfhydrylase; OAS, *O*-acetyl-L-serine; PLP, pyridoxal 5′-phosphate; β-TRPS, β-subunit of tryptophan synthase; TNB, 5-thio-2-nitrobenzoate; Hepes, *N*-(2-hydroxyethyl)piperazine-*N*′-2-ethanesulfonic acid; Mes, 2-(*N*-morpholino)ethanesulfonic acid; Mops, 3-(*N*-morpholino)propanesulfonic acid; Ches, 2-(*N*-cyclohexylamino)ethanesulfonic acid; Caps, 3-(*N*- cyclohexylamino)propanesulfonic acid.

10.1021/bi0268044 CCC: $25.00
Published on Web 12/10/2002

Scheme 1: Reaction Catalyzed by OASS-A

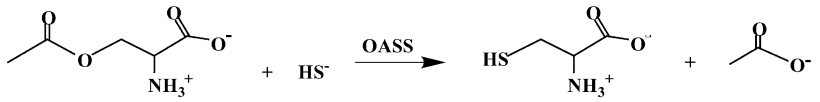

Scheme 2: Proposed Reaction Pathway for a PLP-Dependent E_1cB or E_2 Mechanism[a]

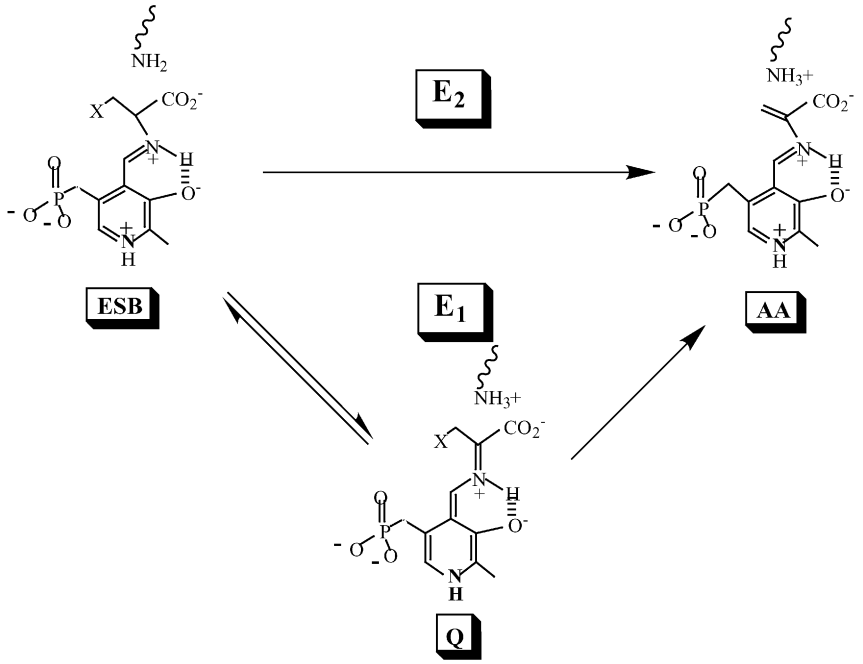

[a] ESB, Q, and AA are the OAS external Schiff base (where X reflects the acetoxy group of OAS), quinonoid intermediate, and the α-aminoacrylate external Schiff base, respectively.

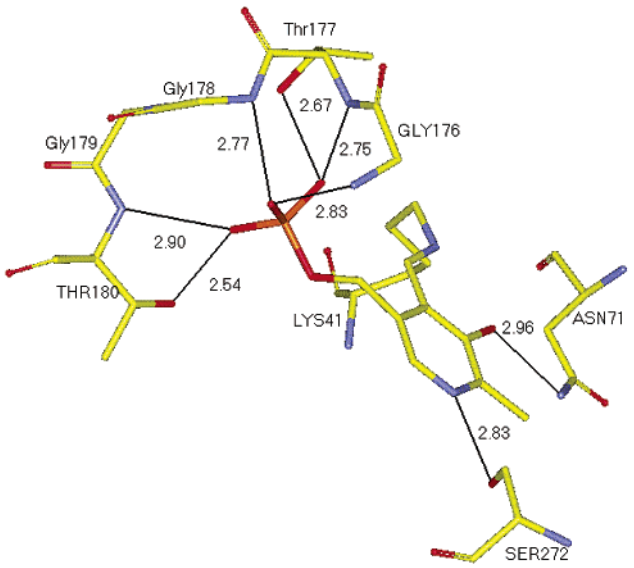

FIGURE 1: View of the active site of OASS-A. PLP is shown in internal Schiff base linkage with lysine 41. The 5′-phosphate is anchored to the glycine 176 to the threonine 180 loop via several hydrogen bonds. Serine 272 is within hydrogen bonding distance to N1 of the pyridinium ring, and O3′ of the pyridinium ring is within hydrogen bonding distance to N71.

There is evidence that in OASS-A the central α,*β*-elimination proceeds via an anti-E_2 mechanism (*4*). The crystal structure of the K41A mutant of OASS-A, with PLP bound to the active site, exists in an active site closed structure with a free methionine from solution in Schiff base linkage with PLP (*5*). In the active site of the mutant enzyme, the methionine side chain extends away from the re-face of PLP toward the entrance of the active site, while the α-proton extends away from the si-face, toward A41, which in the wild type is the location of K41, the general base. Thus, the enzyme catalyzes an anti elimination, as expected for an E_2 reaction.

Serine 272 could stabilize a quinonoid intermediate as required in the stepwise E_1cb reaction, Scheme 2. The quinonoid intermediate can be detected as a band near 500 nm in the presteady state in the elimination direction when leaving group elimination is slow and in the opposite reaction direction when protonation of the α-carbon is slow. The reaction catalyzed by the *β*-subunit of tryptophan synthase (*β*TRPS) is known to proceed via an E_1cB and also has a serine (S377) hydrogen-bonded to N1 of the pyridine ring (*6*, *7*). The quinonoid intermediate is transiently observed in the *β*TRPS reaction, suggesting that the protonated N1 of the PLP donates a hydrogen bond to a lone pair on S377 (*4*). In the case of OASS-A, abstraction of the α-proton is slow, but the quinonoid intermediate is not observed in either reaction direction (*4*). In retrospect, it is not surprising that elimination of hydroxide in the *β*TRPS reaction, which requires protonation, might proceed via an E_1cB reaction, while elimination of the stable acetate moiety in the OASS-A reaction might proceed via an E_2 reaction.

To test the proposed E_2 reaction catalyzed by OASS-A, the active site serine was changed to alanine and aspartate. Similar experiments carried out with the S377D mutant of *β*TRPS resulted in stabilization of the quinonoid intermediate. A prominent band at 500 nm is observed under equilibrium

conditions when L-serine is mixed with βTRPS S377D, consistent with the expected increased stability of the intermediate based on the stronger ionic interaction between the ionized form of N1 and the β-carboxylate of aspartate (*8*). In this manuscript, we report that although mutation of S272 has some effect on the OASS reaction, the enzyme is still quite active. Data are discussed in view of the PLP-dependent elimination reaction.

MATERIALS AND METHODS

Chemicals. Buffers were obtained from Research Organics. Deuterium oxide was from Cambridge isotope laboratories. All other chemicals were purchased from Sigma and were of the highest purity available. The wild-type and mutant enzymes were purified according to the procedure developed by Hara et al. (*9*) and adapted for HPLC by Tai et al. (*10*).

L-Serine-2d was prepared according to Hwang et al. (*11*), using the OASS-mediated exchange of the α-proton in D_2O. The atom % deuterium in the final product was determined using ^{1}H NMR. Acetylation of L-serine-2d was performed according to Sheehan et al. (*12*).

Spectral Studies. All spectra were collected at room temperature using quartz cuvettes with a path length of 1 cm and an inner volume of 1 mL. UV−vis spectra were measured using a Hewlett-Packard 8453 diode array spectrophotometer at pH 7, 100 mM Hepes with an enzyme concentration of 800 μg/mL. For all absorbance readings, spectrophotometers were blanked against a standard containing all components except the absorbing species.

Circular dichroic (CD) spectra were collected using an Aviv 62DS spectropolarimeter. Far-UV spectra (190−280 nm) were recorded using a 0.2-cm path length quartz cuvette with an inner volume of 0.5 mL. Phosphate buffer at pH 7 and a concentration of 10 mM was used. The protein concentration was 100 μg/mL. Visible spectra were obtained in a similar manner with the exception that 100 mM Hepes, pH 7 was used, and the enzyme concentration was 0.6 mg/mL. All spectra are the average of three readings, scanned at 1-nm intervals. Buffer blanks were subtracted from the respective samples. During the experiments, the temperature was maintained at 25 °C, and the reaction chamber and lamp were flushed with nitrogen. CD experiments were performed in the same cuvette, which was extensively rinsed and dried between experiments.

Fluorescence spectra were collected on an SLM 8100 spectrophotometer, using quartz cuvettes with an inner volume of 3 mL. The temperature of the reaction chamber was maintained at 25 °C during the experiments. The excitation wavelength was set to 298 nm since at this value unperturbed tryptophan emission spectra are obtained for the OASS-A fluorescence at high quantum yield (*13*). Emission spectra were collected between 320 and 600 nm at 2-nm intervals. The excitation and emission slits were set to an 8-nm bandwidth. Blank spectra, containing all components except enzyme, were collected and subtracted from sample spectra.

Initial Velocity Studies. Initial velocity studies were carried out using OAS and 5′-thio-2-nitrobenzoate (TNB) (*10*). The initial rate was measured by monitoring the disappearance of TNB at 412 nm (ϵ_{412} = 13 600 M^{-1} cm^{-1}). The initial rate was measured as a function of OAS at several different fixed concentrations of TNB and OAS unless otherwise indicated. With few exceptions, experiments were carried out using the following buffers at a final concentration of 100 mM: Mes (pH 5.5−6.5); Mops (pH 7−7.5); Hepes (pH 8); Ches (pH 9); and Caps (pH 10−10.5). All buffers were titrated with KOH. For all experiments, the pH of the solutions was recorded before and after the reaction.

Rapid-Scanning Stopped-Flow Studies. Presteady-state kinetic measurements on the time scale of seconds were recorded with an OLIS-RSM 1000 stopped-flow spectrophotometer. Sample solutions were prepared in two syringes with the same pH and buffer concentration. One syringe additionally contained the enzyme with a concentration no lower than 20 μM, while the second syringe contained substrate. The formation of the aminoacrylate intermediate was monitored as the increase in absorbance at 470 nm. First-order data were fitted to eq 1 to obtain rate constants.

$$A_t = A_0 \exp(-k_1 \cdot t) + B_0 \quad (1)$$

In eq 1, A_t is the absorbance at time t, A_0 is the absorbance at time zero, and B_0 corrects for the background absorbance.

Primary Deuterium Isotope Effects. Measurements of the primary deuterium isotope effect on α-H/D abstraction from OAS, catalyzed by the S272A mutant of OASS-A were performed by presteady-state kinetic experiments at pH 6.15. The S272A mutant of OASS-A was used at a concentration of 20 μM. The concentration of OAS-2-H(D) was varied from 20 μM to 5 mM. The concentration of OAS stock solutions was determined using wild-type enzyme in excess over OAS and calculating the concentration of OAS from the change in absorbance at 470 nm using an extinction coefficient of 9760 M^{-1} cm^{-1} (*14*). Rate constants were calculated as above.

Data Processing. Reciprocal initial velocities were plotted as a function of reciprocal substrate concentration, and all plots were linear. Appropriate rate equations were fitted to the data using a nonlinear least squares process and FORTRAN programs developed by Cleland (*15*). Substrate saturation curves were fitted using eq 2. Primary kinetic deuterium isotope effects, ^DV and $^D(V/K_{\beta CA})$, were calculated by direct comparison of initial rates using eq 3.

$$v = VA/(K_a + A) \quad (2)$$

$$v = VA/[K_a(1 + F_i E_{V/K}) + A(1 + F_i E_V)] \quad (3)$$

In eqs 2 and 3, v is the initial velocity, V is the maximum velocity, K_a is the Michaelis constant for A, and F_i is the fraction of deuterium label in the substrate. E_V and $E_{V/K}$ are the isotope effects on the first and second-order rate constants minus one.

RESULTS

CD Spectroscopy. Far-UV and visible CD spectra of the S272A mutant of OASS-A were recorded in the absence and presence of L-serine, cysteine, and OAS, Figure 2. The spectrum of the unliganded S272A mutant enzyme is identical to that of the wild-type OASS-A, indicating that the mutation of S272 has not altered the overall structure of the protein and that changes are restricted to the local environment of the active site. Addition of OAS, L-cysteine,

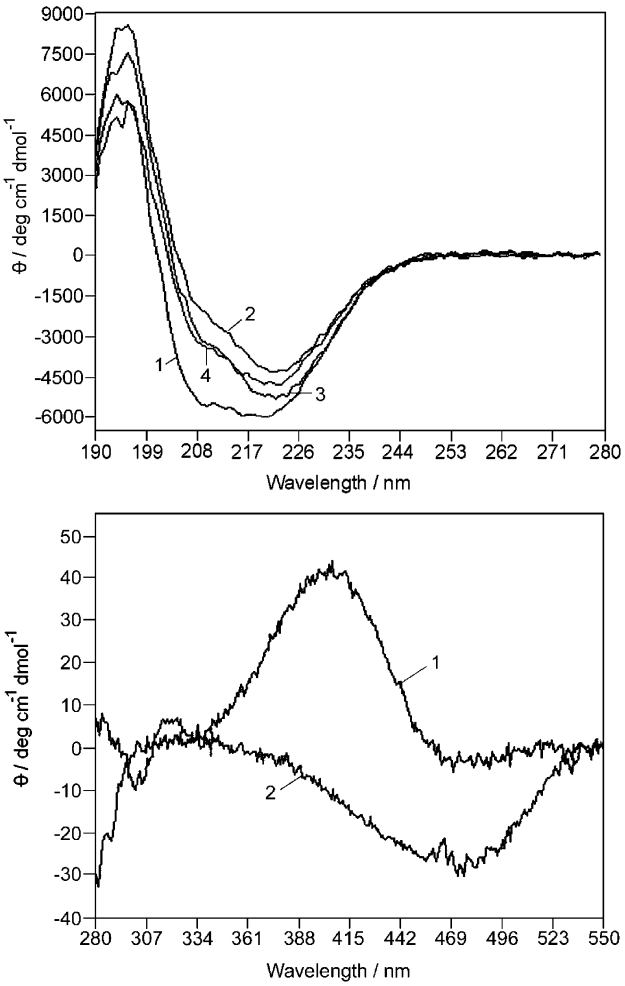

FIGURE 2: Far-UV and visible CD spectra of the S272A mutant of OASS-A. (A) Far-UV CD spectra of enzyme alone (1) and in the presence of 1 mM OAS (2), 150 mM L-serine (3), and 15 mM L-cysteine (4). (B) Visible CD spectra of enzyme alone (1) and in the presence of 1 mM OAS (2). Spectra were measured at pH 7, 10 mM phosphate at 25 °C using a 0.2-cm path and OASS-A concentrations of 100 μg/mL for the far-UV and 0.6 mg/mL for the visible range.

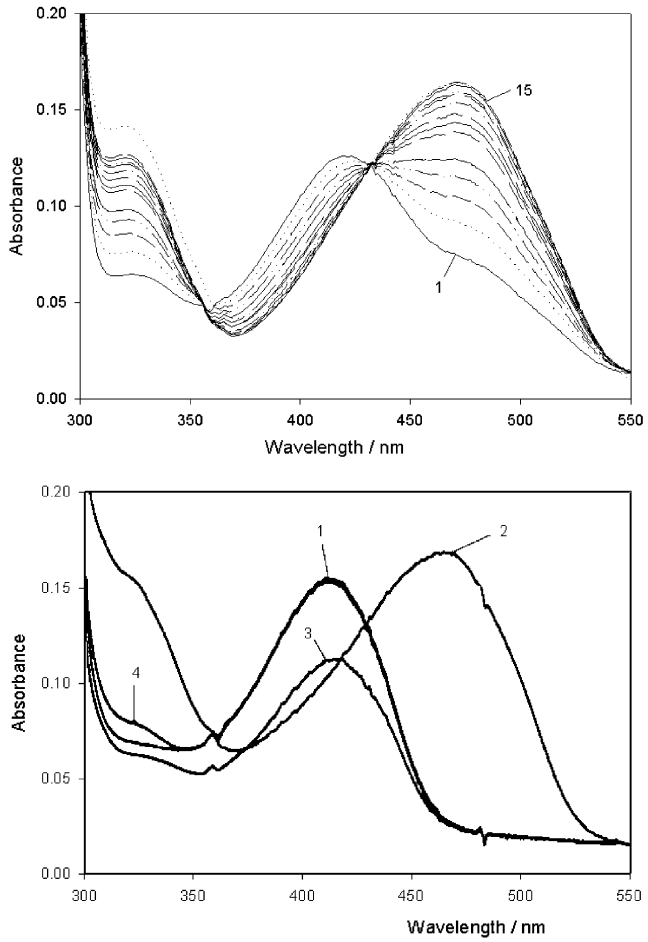

FIGURE 3: UV−vis absorbance spectra of the S272A and S272D mutant enzymes. (A) Titration of the S272A mutant enzyme with OAS to generate the α-aminoacrylate external Schiff base. Addition of 1mM OAS to the S272A mutant of OASS-A (20 μM) at pH 6 results in the slow formation of absorbance bands at 470 and 320 nm, reflecting the α-aminoacrylate external Schiff base. The first spectrum was collected at about 5 s after mixing, while spectrum 15 was recorded after approximately 45 min. The tight isosbestic points for all but the last spectrum reflects the simple interconversion of the OAS external Schiff base (418 nm) and the α-aminoacrylate external Schiff base (330 and 470 nm). The deviation noted for the last spectrum suggests the formation of free enzyme as the α-aminoacrylate intermediate decay. (B) UV−vis absorbance spectra of the S272D mutant of OASS-A. The spectra are for the S272D mutant enzyme alone (1), in the presence of 1 mM OAS (2), in the presence of 15 mM L-cysteine (3), and with 150 mM L-serine (4). All spectra were collected with an enzyme concentration of 550 μg/mL at 25 °C and pH 7, 100 mM Hepes for the S272A mutant enzyme and pH 6.5, 100 mM Hepes for the S272D mutant enzyme.

or L-serine gives an increase in intensity in the 208−215 nm region, consistent with results obtained for the wild-type enzyme (*16*). Data suggest a conformational change in the active site upon substrate binding.

In the visible region, the free S272A mutant enzyme exhibits a positive Cotton effect, which is maximal at 412 nm. The induced CD spectrum results from interactions between the cofactor and the apoenzyme, resulting from π to π* transitions of the PLP cofactor in the protonated Schiff base (*17*). Addition of L-serine or L-cysteine causes the λ_{max} value to shift from 412 to 418 nm, indicating the formation of the external Schiff base, and the maximum ellipticity occurs at the same wavelength for the wild-type and S272A mutant enzymes (data not shown). However, the molar ellipticity at 412 nm for free mutant enzyme is only 50% of that observed for wild-type enzyme, Figure 2, suggesting that the cofactor is bound somewhat differently in the active sites of these two enzymes. Addition of OAS to the S272A mutant enzyme results in the formation of an α-aminoacrylate intermediate, which generates a negative Cotton effect that is maximal at 470 nm. At a given enzyme concentration, the molar ellipticity values for the wild-type enzyme in the absence and presence of OAS are of equal magnitude but with opposite sign (*16*). The S272A mutant enzyme gives qualitatively identical behavior, but the ratio of the molar ellipticities is less than 1 for the 470 and 412 nm bands.

UV−Vis Spectroscopy. UV−vis spectra were collected for the enzyme with and without OAS, L-cysteine, and L-serine. As for wild-type OASS-A (*16*), addition of OAS to the enzyme gives a decrease in absorbance at 412 nm concomitant with increases at 330 and 470 nm, Figure 3. Data are consistent with the formation of the α-aminoacrylate external Schiff base. The aminoacrylate Schiff base disappears with time in a first-order process, indicating the presence of an OAS/acetate lyase activity, as observed for the wild-type enzyme. The rate of formation of the amino-

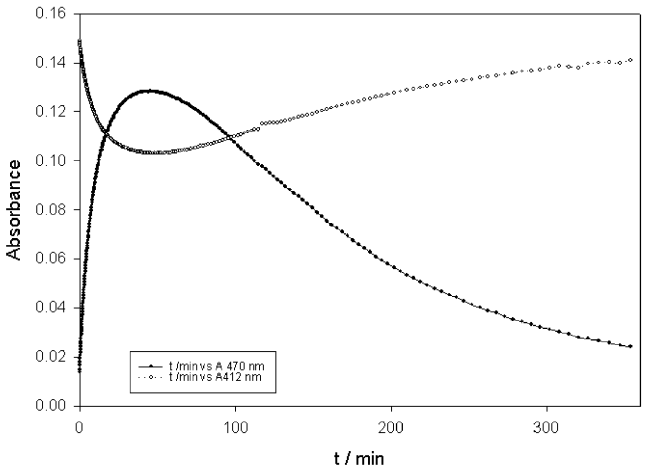

FIGURE 4: Time courses for the S272A-catalyzed formation and decay of the α-aminoacrylate intermediate. Formation (A_{470}) and the concomitant decay and reformation of free enzyme (A_{412}) were monitored at pH 6, 100 mM Mes and 25 °C. Addition of 20 μM OAS to an equimolar amount of the S272A mutant enzyme results in the time courses shown. The time courses reflect the sum of two first-order processes with identical rate constants obtained from the changes in 412 and 470 nm, respectively.

acrylate intermediate is decreased in the S272A mutant enzyme. The appearance and disappearance of absorbance at 470 nm, reflecting formation and disappearance of the aminoacrylate intermediate, can be observed over the steady-state time scale as the sum of two first order rates, Figure 4. The changes occur with the same rate constant as does the disappearance of absorbance at 412 nm, reflecting disappearance of the internal Schiff base. The S272D mutant enzyme gives spectra that are qualitatively identical to those of the S272A mutant and wild-type enzymes, Figure 3.

Although the UV−vis spectra for both mutant enzymes is pH independent from 6 to 9, the rate constants measured from time courses such as those shown in Figure 4 are pH dependent. The disappearance of 470 nm absorbance is a monitor of the OAS/acetate lyase activity. The α-aminoacrylate intermediate was prepared by mixing equimolar amounts of the mutant enzyme and OAS. The first-order decay of the 470 nm absorbance band was measured, and this was carried out as a function of pH. The log of the first-order rate constant versus pH is shown in Figure 5. The rate constant increases with pH and becomes pH independent above pH 9, reflecting the protonation state of the ϵ-amino group of K41 in the active site (*18*). At low pH the rate also becomes pH independent, which is unexpected since no other ionizable residue is found in the active site, and no substrate group is known to require protonation to undergo this reaction.

Titration of the S272A mutant enzyme with L-cysteine from zero to saturation causes a shift of the maximum absorbance band from 412 to 418 nm, Figure 6, with concomitant increases in the absorbance at 330 and 470 nm. The 418 nm band is identical to that observed with the wild-type enzyme, while the 330 and 470 nm bands are not observed with wild-type enzyme in the presence of L-cysteine (*16*). Data suggest that elimination of bisulfide occurs and that the α-aminoacrylate external Schiff base is in equilibrium with the cysteine external Schiff base. As stated above, the α-aminoacrylate external Schiff base is unstable, so that over time the spectrum decays to that of the free enzyme. Similar

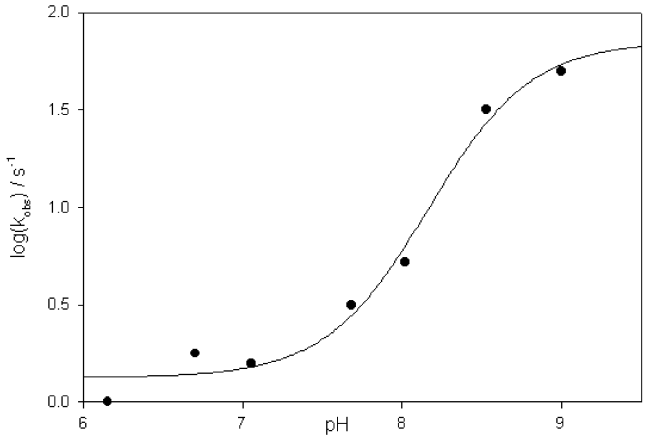

FIGURE 5: Plot of the pH dependence of the rate constant for decay of the α-aminoacrylate intermediate for the S272A mutant enzyme. The rate constant is pH independent at low and high pH. A pK of 8.2 ± 0.1 is estimated from the decrease in the rate constant from pH 9 to 7.5.

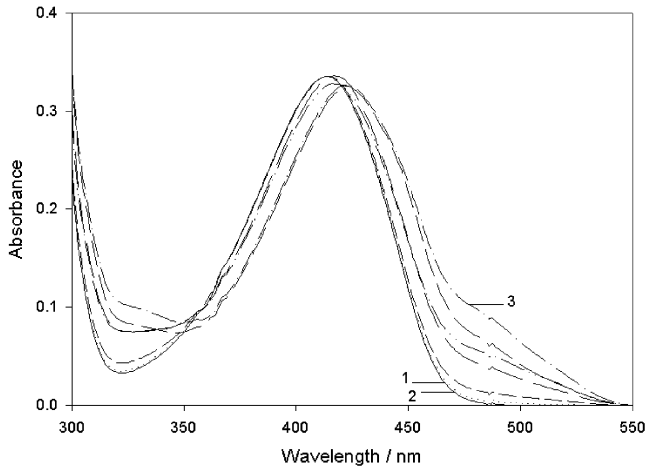

FIGURE 6: Titration of the S272A mutant enzyme with L-cysteine. Spectra were measured with 1.25 mg/mL S272A at pH 9, 100 mM Ches and 25 °C. Spectra are for the S272A mutant enzyme alone (1) and in the presence of increasing concentrations of L-cysteine. Spectra marked 2 and 3 are for 10 and 500 μM L-cysteine, respectively. The lack of clear isosbestic points is consistent with the presence of multiple species.

changes in the spectrum of the S272A mutant enzyme are observed upon addition of L-serine (data not shown). The shift from 412 to 418 nm is accompanied by a significant decrease in absorbance, while formation of the α-aminoacrylate intermediate is manifested as an increase in the 330 and 470 nm bands. Again, the 330 and 470 nm bands are not observed with the wild-type enzyme (*16*). (The lack of clear isosbestic points between the peaks indicates that the internal and external Schiff bases as well as the aminoacrylate form exist at equilibrium.) The rate of formation of α-aminoacrylate intermediate can be seen upon mixing serine and the S272A mutant enzyme under equilibrium conditions, a dramatic increase as compared to wild-type enzyme, which has a rate of days^{-1} with serine as a substrate (*19*). The K_d for the serine external Schiff base at pH 10.5 was determined from the fractional change of the absorbance at 320 nm as 17.2 mM, which can be compared to the value of 4.2 mM measured for the wild-type enzyme at pH 9.5 (*16*).

Fluorescence Spectroscopy. Emission spectra for enzyme were recorded with the excitation monochromator set at 298

Table 1: Steady-State Kinetic Parameters for Wild-Type and Mutant Enzymes

parameter	wild type[a]	S272A[b]	S272D[c]
V/E_t (s^{-1})	0.56 ± 0.08	0.007 ± 0.001	0.016 ± 0.001
$V/K_{OAS}E_t$ ($M^{-1}\,s^{-1}$)	37 ± 5	11.3 ± 0.2	43 ± 15
$V/K_{TNB}E_t$ ($M^{-1}\,s^{-1}$)	950 ± 60	29 ± 1	520 ± 60
K_{OAS} (mM)	15 ± 3	0.6 ± 0.2	0.4 ± 0.2
K_{TNB} (mM)	0.6 ± 0.1	0.24 ± 0.050	0.03 ± 0.005

[a] From ref *10*. [b] Measured at pH 6. [c] Measured at pH 6.5.

nm in the absence and presence of 10 mM OAS, 150 mM serine, or 15 mM cysteine (data not shown). In the absence of ligands, the S272A mutant enzyme exhibits an emission maximum at 335 nm, similar to the value of 337 nm observed for the wild-type enzyme (*13*). The wild-type enzyme also exhibits significant fluorescence at 500 nm upon excitation at 298 nm resulting from triplet to singlet Förster energy transfer from W162 to the PLP cofactor (*13*, *20*, *21*). The S272A mutant enzyme, however, gives barely detectable fluorescence at 500 nm. Addition of either L-serine or L-cysteine to the S272A mutant enzyme results in an increase in the emission at 500 nm, with the intensity in the presence of the cysteine external Schiff base approximately twice that in the presence of the serine external Schiff base. Addition of OAS eliminates the 500 nm band. All results are qualitatively identical to those obtained with the wild-type enzyme.

Initial Velocity Studies. Steady-state kinetic parameters are shown in Table 1. A slight decrease is observed in $V/K_{OAS}E_t$ for both the S272A and the S272D mutant enzymes as compared to that of the wild-type enzyme, which reflects the first half-reaction for OASS-A. Mutation of S272 does not affect the ability of the enzyme to catalyze its reaction. The V/E_t for the S272A and S272D mutant enzymes decreases by 80 and 35fold, respectively, and the greatest majority of this decrease is mirrored in the decreased value of $V/K_{TNB}E_t$.

Primary Isotope Effects. Noncompetitive measurements of the primary deuterium isotope effect on α-deprotonation of OAS by the S272A mutant enzyme were performed as presteady-state experiments at pH 6, using a diode array spectrophotometer. Reactions were initiated by quickly mixing enzyme and substrate in a tandem cuvette. Pseudo-first-order reaction rates of the formation of the α-amino-acrylate intermediate were measured by monitoring the increase in absorbance at 470 nm as a function of OAS-2-(H,D). An isotope effect of two is estimated, consistent with a rate-limiting elimination reaction.

Presteady-State Kinetics. Kinetic parameters for the formation of the α-aminoacrylate intermediate in the first half-reaction of the S272A mutant enzyme reaction were obtained as a function of pH. A double reciprocal plot of the first-order rate constant versus the concentration of OAS is shown in Figure 7. The plot is suggestive of negative cooperativity. The $S_{0.5}$, the concentration of OAS required to give one-half of the maximum rate, was obtained by plotting the data as a Hill plot (Figure 7, inset) according to

$$\log\{k_{obs}/(k_{AA} - v)\} = n_H \log[OAS] - \log S_{0.5} \quad (4)$$

In eq 4, k_{obs} is the first-order rate constant measured at a specific concentration of OAS, k_{AA} is the maximum rate, n_H is the Hill number, and $S_{0.5}$ is the substrate concentration that gives 1/2 the maximum rate. A Hill number of 0.5 is obtained as the slope of the linear function, which suggests negative cooperativity, likely the result of the coexistence of either different enzyme forms or different orientations of the cofactor in the active site. This aspect will require further study.

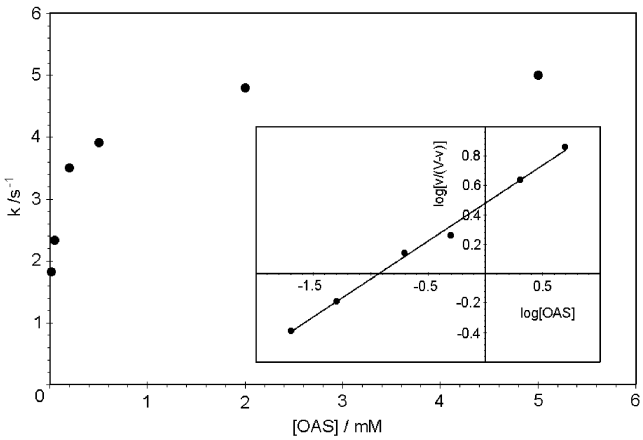

FIGURE 7: Saturation curve for OAS. The first-order rate of the formation of the aminoacrylate intermediate was measured at pH 7, 100 mM Hepes and 25 °C. Inset: A Hill plot exhibiting a slope of about 0.5 indicative of negative cooperativity.

Table 2: Presteady-State Kinetic Data Obtained for the Wild-Type and S272A Mutant Enzymes[a]

parameter	wild type[b]	S272A
k_{AA} (s^{-1})	300 ± 30	6.0 ± 0.6
K_{ESB} (mM)	5.0 ± 0.5	NA
$S_{0.5}$ OAS (mM)	NA	0.32 ± 0.02
k_{AA}/K_{ESB} ($M^{-1}\,s^{-1}$)	$(6.0 \pm 0.8) \times 10^4$	NA
$k_{AA}/K_{S0.5}$ ($M^{-1}\,s^{-1}$)	NA	$(1.9 \pm 0.1) \times 10^4$

[a] Data were obtained at 25 °C and pH 7, 100 mM Hepes; NA = not applicable. [b] From ref *22*.

The kinetic parameters for the S272A mutant enzyme are shown in Table 2. For comparison, the values for wild-type enzyme are also given. Maximum rates (k_{AA}) were obtained by fitting the data using eq 2. For data analysis, kinetic parameters of the S272A mutant enzyme at pH 7 were used for comparison since errors on these data are the lowest. Since the wild-type reaction is too fast for data acquisition at high pH, data can only be obtained at pH 6.5 or below.

DISCUSSION

Structural Integrity of the Mutant Enzymes. The mutant enzymes are expressed in amounts equivalent to and purified using the same procedure as the wild-type enzyme. The far-UV CD spectra of the mutant enzymes are identical to that of the wild-type enzyme in the absence and presence of OAS or cysteine or serine, indicating similar global structures. Both mutant enzymes have UV−vis spectra in the absence and presence of OAS that are identical to those of the wild-type enzyme. The λ_{max} of the emission spectra for intrinsic tryptophan fluorescence is identical for wild-type and mutant enzymes. Both mutant enzymes are active. On the basis of the above, the global structure of the mutant enzymes is identical to that of the wild-type enzyme, and any changes resulting from the mutations must be localized to the active site.

Spectral Studies. Equilibrium spectral studies provide qualitative and quantitative data that the S272 mutant enzymes catalyze the synthesis of cysteine from OAS and bisulfide. Addition of OAS to the mutant enzymes results in the formation of the α-aminoacrylate Schiff base intermediate, and addition of bisulfide to the intermediate regenerates the free enzyme. The slight amount of long wavelength fluorescence at 500 nm is eliminated when OAS is mixed with the mutant enzymes as a result of converting the internal Schiff base (412 nm) to the α-aminoacrylate Schiff base intermediate (470 nm). Finally, an increase in the intensity of the 208−215 nm far-UV CD band (reflecting coil and β-structure) is observed upon addition of OAS, cysteine, or serine to the mutant enzymes and inducing a conformational change to close the active site. All of the above are observed with the wild-type enzyme (*13*, *16*, *18*).

Spectral data also indicate differences in the orientation of the active site PLP in wild-type and mutant enzymes. Induced CD signals in the visible region are an indicator of the asymmetry of the interaction of protein and chromophore. As stated in the Results, the molar ellipticity of the visible induced CD bands in the mutant enzymes are lower than those observed in the wild-type enzyme. In addition, the relative intensities of the visible bands in the mutant enzymes differ as compared to the same ratios in the wild-type enzyme. Although the same spectral shifts in the UV−vis absorbance spectra are observed for mutant and wild-type enzymes, the aminoacrylate intermediate is observed upon addition of cysteine or serine to the mutant enzymes but not the wild-type enzyme. The triplet to singlet Förster energy transfer from W162 to the PLP cofactor is dependent on the relative orientation on the acceptor and donor and is barely detectable at 500 nm in the mutant enzymes. Addition of either L-serine or L-cysteine to the S272A mutant enzyme results in an increase in the emission at 500 nm but with much lower intensity as compared to the wild-type enzyme.

Although the group that hydrogen-bonds to N1 of the PLP cofactor is eliminated (S272A) or changed to a residue that could generate a stronger ionic interaction (S272D), the mutant enzymes still function under equilibrium conditions in a manner nearly identical to the wild-type enzyme. All of the differences discussed above can be attributed to a difference in the orientation of the cofactor. The failure to observe the quinonoid intermediate in either reaction direction with the S272D mutant enzyme and the capability of the S272A mutant to catalyze the reaction are in agreement with the proposed anti-E_2 reaction. A similar mutation made in β-TRPS (S377D) does result in formation of a stable quinonoid intermediate under equilibrium conditions, consistent with the expected increased stability of the intermediate based on the stronger ionic interaction between the ionized form of N1 and the β-carboxylate of aspartate (*8*). These experimental results highlight the difference in OASS-A and β-TRPS, which catalyze similar reactions.

Kinetic Studies. As discussed above, the S272A and S272D enzymes are capable of catalyzing the overall reaction for cysteine synthesis. The proof of how well the enzymes catalyze the reaction, however, must come from kinetic studies. The data in Table 1 indicate that both mutant enzymes are as efficient as the wild-type enzyme in catalyzing the first half-reaction (i.e., the conversion of OAS and the internal aldimine of OASS-A to acetate and the α-aminoacrylate external Schiff base). The V/K for the second half-reaction is decreased significantly (32-fold, S272A; 1.8-fold, S272D), and this is reflected in the turnover number for the mutant enzymes (80-fold, S272A; 35-fold, S272D). It is clear that even taking into account the decrease in the above rate constants, the mutant enzymes are still very good catalysts.

A closer look at the parameters measured for the first half-reaction provides additional information. In addition to the decrease in V/E_t, K_{OAS} decreases 25- and 35-fold, respectively, for the S272A and S272D mutant enzymes. The decrease in K_m is what compensates for the decrease in V/E_t, to give little to no net change in V/K. A similar compensatory effect, although not as substantial, is also observed for the second half-reaction.

In the presteady state, Table 2, the maximum rate of formation of the aminoacrylate intermediate (k_{AA}) is about 50-fold higher for the wild-type enzyme than it is for the S272A mutant enzyme. The $S_{0.5}$ value for the S272A mutant enzyme is about 17-fold lower than the external Schiff base dissociation constant measured for the wild-type enzyme, consistent with an increase in substrate affinity of the S272A mutant enzyme. The apparent second-order rate constant ($k_{AA}/S_{0.5}$) for the S272A mutant enzyme is about 3-fold lower than that (k_{AA}/K_{ESB}) measured for the wild-type enzyme, in agreement with data from the initial velocity studies. A simplified mechanism for the first half of the OASS-A reaction is given below.

$$E \underset{k_2}{\overset{k_1 A}{\rightleftharpoons}} EOAS \underset{k_4}{\overset{k_3}{\rightleftharpoons}} ESB \xrightarrow{k_5} F$$

For this mechanism, the second-order rate constant V/K_{OAS} can be expressed in terms of microscopic rate constants as shown in

$$\frac{V}{K_{OAS}} = \frac{k_1 k_3 k_5}{k_2 k_4 + k_2 k_5 + k_3 k_5} \tag{5}$$

A primary deuterium isotope effect of two is observed for the elimination reaction, and thus the formation of the α-aminoacrylate intermediate ($k_5 = k_{AA}$) is the rate-limiting step in this mechanism. The value of k_5 is thus smaller than k_2, k_3, and k_4, and eq 5 reduces to

$$\frac{V}{K_{OAS}} = \frac{k_1 k_3 k_5}{k_2 k_4} = \frac{k_5}{K_{ESB}} \tag{6}$$

Thus, the lack of decrease in the second-order rate constant, $V/K_{OAS,}$ for the mutant enzymes is a compensatory effect. The decrease in k_5 of 80- and 35-fold is compensated for by a decrease in K_{ESB}. The decrease in k_5 and K_{ESB} can be explained by a change in orientation of the bound cofactor, as documented via the spectral studies discussed above. In the case of the S272A mutant enzyme, this is likely a consequence of a tilt in the ring as a result of elimination of the hydrogen bond from S272 to N1 of PLP. It is proposed that the new position of the imine is more easily attacked to trap the incoming amino acid reactant as the external Schiff base. In the case of the S272D mutant enzyme, it is likely that the same explanation applies since the changes in kinetic parameters are in the same direction as those measured for

the S272A mutant enzyme, even though the β-carboxylate of the new aspartate will hydrogen-bond N1 of the PLP.

*O-Acetyl-*L*-serine: Acetate Lyase Activity and the pK for K41*. In this reaction, the displacement of α-aminoacrylate from its external Schiff base with PLP by K41 occurs, regenerating the internal Schiff base form of the enzyme (*18*). The aminoacrylate produced is nonenzymatically hydrolyzed to pyruvate and ammonia. In order for the reaction to occur, the ϵ-amine of K41 must be unprotonated. The pH dependence of the lyase reaction has been used to estimate a value of 8.2 for the wild-type enzyme (*18*). Similar experiments carried out with the S272A mutant enzyme give an identical p*K* of 8.2 ± 0.1. Thus, once the aminoacrylate intermediate has been formed in the elimination reaction, the p*K* of K41, which acts as a general acid in the second half-reaction, is unchanged.

The pH independence of the reaction rate at low pH, Figure 5, suggests that some other process that also regenerates free enzyme is observed once the rate of the lyase has decreased by a factor of 50. Since the rate is pH independent, an acid−base mechanism can likely be ruled out. It is possible that nucleophilic attack of a water molecule on the β-carbon of the α-aminoacrylate Schiff base occurs, forming the serine external Schiff base. L-Serine has very low affinity for the wild-type enzyme at pH 6.5 or below (*16*). Given a 4-fold decrease in the K_d for the serine external Schiff base in the S272A mutant enzyme as compared to the wild-type enzyme, dissociation of serine can be seen as the driving force for this process.

REFERENCES

1. Becker, M. A., Kredich, N. M., and Tomkins, G. M. (1969) *J. Biol. Chem. 244*, 2418−2427.
2. Burkhard, P., Rao, G. S. J., Hoehenester, E., Schnackerz, K. D., Cook, P. F., and Jansonius, J. N. (1998) *J. Mol. Biol. 283*, 121−133.
3. Rege, V. D., Tai, C.-H., Kredich, N. M., Karsten, W. E., Schnackerz, K. D., and Cook, P. F. (1996) *Biochemistry 35*, 13485−13493.
4. Tai, C.-H., and Cook, P. F. (2001) *Acc. Chem. Res. 34*, 49−59.
5. Burkhard, P., Tai, C.-H., Ristroph, C., Cook, P. F., and Jansonius, J. N. (1999) *J. Mol. Biol. 291*, 941−953.
6. Goldberg, M. E., and Baldwin, R. L. (1967) *Biochemistry 6*, 2113-2119.
7. Schleicher, E., Mascaro, K., Potts, R., Mann, D. R., and Floss, H. G. (1976) *J. Am. Chem. Soc. 98*, 1043−1044.
8. Jhee, K.-H., Yang, L.-H., Ahmed, S. A., McPhie, P., Rowlett, R., and Miles, E. W. (1998) *J. Biol. Chem. 273*, 11417−11422.
9. Hara, S., Payne, M. A., Schnackarz, K. D., and Cook, P. F. (1990) *Protein Expression Purif. 1*, 70−76.
10. Tai, C.-H., Nalabolu, S. R., Jacobson, T. M., Minter, D. E., and Cook, P. F. (1993) *Biochemistry 32*, 6433−6442.
11. Hwang, C.-C., Woehl, E. U., Dunn, M. F., and Cook, P. F. (1996) *Biochemistry 35*, 6358−6365.
12. Sheehan, J. C., Goodman, M., and Hess, G. P. (1956) *J. Am. Chem. Soc. 78*, 1367−1369.
13. McClure, G. D., Jr., and Cook, P. F. (1994) *Biochemistry 33*, 1647−1683.
14. Cook, P. F., and Wedding, R. T. (1976) *J. Biol. Chem. 251*, 2023−2029.
15. Cleland, W. W. (1979) *Anal. Biochem. 99*, 142−145.
16. Schnackerz, K. D., Tai, C.-H., Simmons, J. W., III, Jacobson, T. M., Rao, G. S. J., and Cook, P. F. (1995) *Biochemistry 34*, 12152−12160.
17. Miles, E. W., and Morkguchi, M. (1977) *J. Biol. Chem. 252*, 6594−6599.
18. Cook, P. F., Hara, S., Nalabolu, S., and Schnackerz, K. D. (1992) *Biochemistry 31*, 2299−2303.
19. Flint, D. H., Tuminello, J. F., and Miller, T. J. (1996) *J. Biol. Chem. 271*, 16053−16067.
20. Strambini, G. B., Cioni, P., and Cook, P. F. (1996) *Biochemistry 35*, 8392−8400.
21. Mozzarelli, A., and Rossi, G. L. (1996) *Annu. Rev. Biophys. Biomol. Struct. 25*, 343−365.
22. Woehl, E. U., Tai, C.-H., Dunn, M. F., and Cook, P. F. (1996) *Biochemistry 35*, 4776−4783.

BI0268044